MAIN LECTURES

ML-01
AGING PROCESSES – MECHANISMS AND QUANTITATIVE CHARACTERIZATION CONCERNING POLYMER STRUCTURE, ANTIOXIDANTS AND CROSSLINKING

ULRICH GIESE*, I. HOMEIER, Y. NAVARRO TORRÉJON, and S. KAUTZ

Deutsches Institut für Kautschuktechnologie e. V., Eupener Str. 33, 30519 Hannover / Germany
Ulrich.Giese@DIKautschuk.de

1. Introduction

The exposure of elastomer components during service against environmental influences like oxygene, temperature, static and dynamic mechanical load or UV-light effects aging processes. Especially chemical changes caused by those influences are responsible for irreversible changes in properties[1]. Depending on the polymer type, on the used crosslinking system and on processing the aging mechanisms lead macroscopically to increasing stiffness and hardness or stickiness[2]. Failures in function of the component are the consequence. Alongside the selection of polymers, the aging process is determined mainly by the use of anti-aging agents – e.g. p-phenylenediamines or by substituted phenols[3,5–8]. This work focuses specifically on temperature dependency, kinetic aspects of thermal-oxidative aging, on the influence of polymer structure, crosslinking density and crosslink structures and on the consumption and mechanistic aspects of antioxidants. The knowledge about kinetics and of the most efficient processes should be used for simulation models in future.

2. Theoretical aspects of thermal-oxidative aging

The chemical aging of polymers in presence of temperature and oxygene is determined by means of a three-phase radical mechanism[9–14]. The chain reaction is terminated by recombination reactions with the formation of stable compounds, such as, for instance, the constitution of C-C or C -O-C bonds from two macroradicals, tantamount to an increase in crosslinking density. An embrittlement of the material is the macroscopic consequence. On the polymer, there is also formation of polar oxygenic side groups, which likewise have a stiffening effect due to inter- and intramolecular interactions. Especially at higher termperatures for some polymers like NR, chain scission can also be observed as a dominant effect, accompanied by elastomer viscosity. The two reaction channels compete with one another, with the polymer configuration (double bonds of the main chain, side groups) playing a more significant role like the nitrile group in the case of NBR[19,20]. The formation of sulfones, sulfonates and sulfates is described for reactions in the area of the sulfur network[21,22].

Antioxidants are usually used to avoid aging processes. The antioxidants have different effectiveness in dependency on their molecular structure, chemical reactivity and diffusion behavior. Considering chemical reaction mechanism in the subject of thermal-oxidative aging two groups of antioxidants are exists, the primary (chain breaking) and secondary antioxidants[10,23–25]

3. Methods and materials

Systematic investigations were performed on the aging stability of uncrosslinked, crosslinked NBR`s (varied in acrylonitrile content) and SBR´s (varied in vinyl content).

Measurements were carried out by means of rheometry, chemiluminescence (CL)[17], ATR-FT-IR spectroscopy, in combination with CL and NMR-relaxation. The characterization of changes in physical properties during aging stress-strain measurements and determination of hardness were used in dependency on aging in ventilated air cabinets up to 1000 h at different temperatures in the range of 80 to 140 °C.

Furthermore the consumption, diffusion and effectiveness of *p*-phenylenediamines as antioxidants were investigated by means of ATR-FT-spectroscopy using a sandwich arrangement of a reservoir for the diffusing substance and a thin layer of the matrix. The calculation of diffusion coefficients bases on the Fick`sch law and the time lag method.

4. Results

4.1. Investigations on uncrosslinked NBRs

The thermal oxidation aging of polydienes is significantly influenced by the double bond concentration in the main chain (1,4 units)[17,18], which is reduced with increasing concentration of the acrylonitrile side groups. So the oxidative stability of the pure polymers after extraction of the stabilizers added by the polymer producers should result in decreasing oxygene induction times (OIT values) in chemiluminescence (CL) measurements. The influence of the ACN-content of extracted NBR's on OIT is shown in scheme 1.

The values in scheme 1 show clearly, that up to 28 % ACN- content the OIT values are increasing against to a limit at 34 % ACN . Depending on the ACN-content the aging resistance is increased by factor appr. 3. This is more or less in line with the expectation, that the OIT is depending on the C=C-double bond concentration in the main chain. Unclear is the situation for the extreme high ACN-content of 34 % and especially of 39 %. May be that reactions of the ACN-groups are responsible. This aspect has to be proven by further investigations by means of FT-IR spectroscopy and model substances, which can be analysed by chromatographic methods.

The temperature dependent investigations of oxidative aging on NBR`s results in decreasing times OIT values with

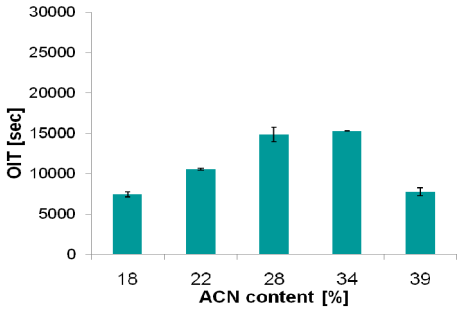

Scheme 1. **OIT-values as function of ACN-content for extracted uncrosslinked NBR`s at 100 °C**

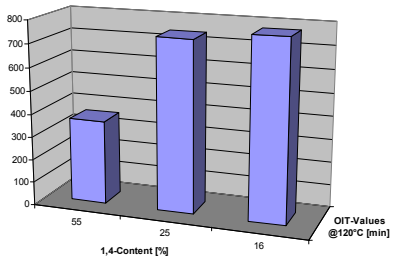

Scheme 3. **OIT-values at 120 °C as function of 1,4 butadiene-content for cured SBR`s with similar crosslinked densities**

increasing temperature in CL measurements as it is shown in the following scheme 2.

The evaluation using the normalized slopes of the first part of the curves[26] and the Arrhenius principle results in activation energies describing the temperature dependency of the aging process are between 37 and 73 kJ mol^{-1}. The values show an increasing tendence with the ACN-content.

4.2. Investigations on crosslinked SBR-rubbers

SBR`with varied vinyl content between 16 % and 55 % were sulfur crosslinked using a unique SEV-system. Fillers were not used. The characterization of the vulcanizates by means of CL results in CL-curves with two maxima, where the first one is considered for the evaluation. The OIT-values result from the cross-section of the tangent with the x-axis by extrapolation from the rising part of the CL-curves. The OIT-values of the SBR`s with different microstructure but with a constant crosslink system at 120 °C are shown in scheme 3.

The OIT-values are increasing with a lower content of C=C-double bonds as it is to be expected considering the reaction mechanism. The reactive part is the hydrogene atom at the allyl-position. This is explained by the inductive effect of the double bond in the chain on the allylic C-H-bond. The bonding energy is lowered in comparison to the C-H-bond in the vinyl-group, so that the abstraction is favoured in this position. An uncertainty of the values is given by the situation, that the material was not extracted and that the crosslink densities are not exactly the same. The variation of the temperature for the aging process in the CL results in decreasing OIT-values with increasing temperature due to the accelerating effect of the temperature for the reaction speed.

In the case of a high C=C-double bond content of the main chain in SBR 1 the activation energy of the reaction controlled by CL is the lowest one. This is in line with the low OIT values for this type of rubber. For SBR 2 and 3 the values are more than double, that means, that a change in temperature has a very high influence on the reaction speed.

4.3. Influence of crosslinking

The OIT values of SBR 2 vulcanizates with low, medium and high crosslink densities are in the range of appr. 400 min at 130 °C, the differences are in the range of the standard deviation of the CL-method, which is in ideal cases appr. 6 %rel. (ref. [27]). The influence of crosslink densities on the thermal oxidative aging was investigated by means of CL, NMR relaxation and physical testing. The OIT values of SBR 2 vulcanizates with low, medium and high crosslink densities (S/CBS 0.5/0.5; 1.5/1.5; 2.5/,2.5) are in the range of appr. 400 min at 130 °C, the differences are in the range of the standard deviation of the CL-method, which is in ideal cases appr. 6 % rel. (ref.[27]). So the crosslink density play a minor role in comparison to the structure of the polymer. The effect of temperature on the aging process in dependency on the crosslink density was characterized by means of the determination of the activation energies using NMR, CL and elongation at break-measurements (scheme 4).

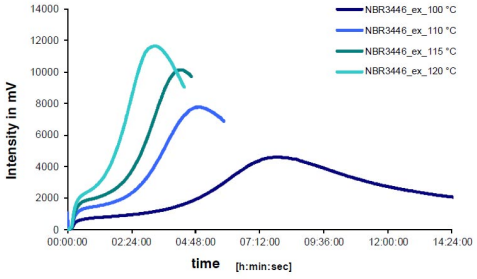

Scheme 2. **OIT-values as function of temperature for extracted uncrosslinked NBR** (ACN-content 28 %)

Table I
Activation energies from CL of the SBR-vulcanizates

Vulcanisate[a]	E_A [kJ mol^{-1}]
SBR 1(15 S, 30 V)	65
SBR 2 (25 S, 63 V)	157
SBR 3 (20 S, 55 V)	135

[a] Crosslinked: 1.5 phr S, 1.5 phr CBS, S = styrene content in %, V = vinyl content in %

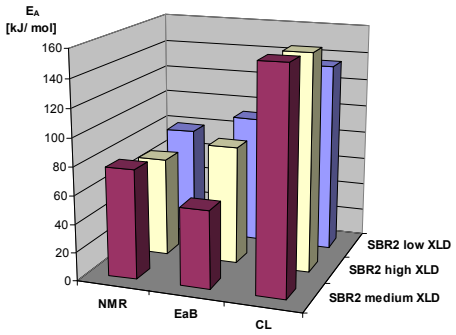

Scheme 4. **Activation energies in dependency of crosslink density for SBR 2 vulcanizates, measured with NMR, EaB = elongation at break and CL**

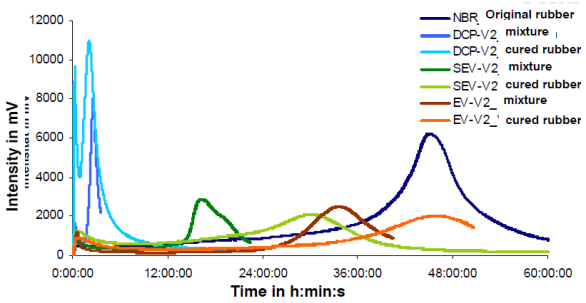

Scheme 5. **CL-curves at 130 °C as function of crosslink structures (EV, SEV and DCP system) at constant XLD for NBR (28 % ACN), uncured NBR compound and original NBR**

In principle the results in scheme 4 are showing, that the values for E_A are depending extremely on the used method measuring different processes. Overall the differences internal of one method are very small. So it is to conclude, that the influence of crosslink density is small in comparison to the effect of the polymer structure and that the different methods show different parts of the oxidation reaction.

The investigations on the influence of crosslink density (XLD) and crosslink structure for NBR (28 % ACN-content) were performed using EV- and SEV systems on two levels (high = V1 and low = V2) with the same XLD per each pair. For comparison a peroxide crosslinked system (Dicumylperoxide = DCP) was used with the same XLDs on the 2 levels as they were prepared for the sulfur systems. The crosslink densities were adjusted by rheometry. The CL-curves at 130 °C for the lower level of XLD with varied crosslink structures incl. the peroxide crosslinked systems shown in scheme 5.

It is obvious, that the mixing process and the vulcanization affect a reduction in the thermal oxidative stability. The maximum of the curve of the original NBR without any treatment is at much higher times than all the others. The reason is, that during processing the material is pre-aged, whereas it is to note, that the antioxidant system added by the manufacturer is consumed during processing. Furthermore the sulfur systems especially the EV-system is much more stable than the DCP-system, which shows, that residual peroxide is a initiator in aging.

4.4. Consumption and effectiveness of antioxidants

The efficiencies of DPPD, 6PPD and 77PD as antioxidants (3 phr per each) were determined using CL with determination of the OIT values of SBR-compounds with different vinyl content of the polymer and of an IR-compound. The highest efficiency calculated from the slope of the graph OIT as f(concentration) shows in all cases the DPPD followed by 6PPD and 77PD. The diffusion coefficients of the antioxidants measured by time lag method and FT-IR spectroscopy are in the range of 4.3 to 0.16 $*10^{-6}$ for all systems, where the values are the lowest one for DPPD and overall they correlate with the chain flexibility of the polymer. So the diffusion is in line with the efficiency, which is depending on the reactivity and on the availability in the system limited by the diffusion speed.

The authors deeply acknowledge the Deutsche Kautschuk Gesellschaft (DKG e.V.) and the Arbeitsgemeinschaft industrieller Forschungsvereinigungen e. V. (AiF) for the support of this work.

REFERENCES

1. DIN 50035 (1972).
2. IUPAC Recommend.-Definitions of Terms Relating to Degrad. Ageing and Rel. Chem. Transf. of Polymers (1996).
3. H. W. Engels, H. Hammer, D. Brück, W. Redetzky: Rubber Chem. Technol. *62*, 609 (1989).
4. J. Sampers: Polym. Deg. Stab. *76*, 455 (2002).
5. D. F. Parra, M. T. De, A. Freire, M.-A. De Paoli: J. Polym. Sci. *75*, 670 (2000).
6. J. C. Ambelang, et al.: Rubber Chem. Technol. *36*, 1497 (1963).
7. J. Boxhammer: Material Test. Prod. Tech. News (Atlas Sun SP) *30*, 1 (2000).
8. R. H. Krüger et al.: Food Additives and Contaminants *22*, 968 (2005).
9. G. Scott: Chemistry and Industry *16*, 271 (1963).
10. G. Scott: *Mechanismen of Polymer Degradation and Stabilisation*, Elsevier Appl. Science, pp. 170, 1990.
11. A. Hoff, S. Jacobsson: J. Appl. Sci. *27*, 2539 (1982).
12. G. Scott: Developments in Polymer Stabilisation, Appl. Science Publishers LTD, pp. 145, 1981.
13. E. A. Snijders, A. Boersma, B. van Baarle, J. Noordermeer: Polymer Degrad. Stab. *89*, 200 (2005).
14. J. L. Bolland: Trans. Faraday Soc. p. 669, 1949.
15. R. W. Keller: Rubber Chem. Technol. *58*, 637 (1985).
16. P. M. Norling, T. C. P. Lee, A. V. Tobolsky: Rubber Chem. Technol. *38*, 1198 (1985).
17. M. Santoso, U. Giese, R. H. Schuster: Rubber Chem. Technol. *81*, 762 (2007).
18. M. Santoso, U. Giese, R. H. Schuster: KGK, Kautsch. Gummi Kunstst. 60, 192 (2007).

19. H. Bender, E. Campomizzi: KGK, Kautsch. Gummi Kunstst. *54*, 14 (2001).
20. S. Bhattacharjee, A. K. Bhowmick, B. N. Avasthi: Polym. Degradation and Stability 31 (1991).
21. G. Scott: Rubber Chem. Technol. *58*, 269 (1985).
22. H. Modrow, R. Zimmer, F. Visel, J. Hormes: KGK, Kautsch. Gummi Kunstst. *53*, 328 (2000).
23. A.G. Ferradino: Rubber Chem. Technol. *76*, 694 (2003).
24. H.-W. Engels: KGK, Kautsch. Gummi Kunstst. *47*, 12 (1994).
25. D. Brück, H.-W. Engels: KGK, Kautsch. Gummi Kunstst. *44*, 1014 (1991).
26. L. Zlatkevich: *Chemiluminescence in Evaluating Thermal Oxidative Stability in Luminescence Techniques in Solid State Polymer Research.* Marcel Dekker, New York 1989.
27. U. Giese, M. Santoso, R. H. Schuster: Lecture: International Rubber Conference (IRC) Nuernberg, July 2009.

ML-02
NANOSCALE STRUCTURE AND PHYSICAL PROPERTIES CHARACTERIZATION FOR SUPER FUEL-EFFICIENT TIRES

TOSHIO NISHI[a] and KEIZO AKUTAGAWA[b]*

[a] *Tokyo Institute of Technology, 2-12-1 Ookayama, Meguro-ku, Tokyo 152-8550, JAPAN,* [b] *Bridgestone Corporation, 3-1-1 Ogawahigashi-cho, Kodaira-shi, Tokyo 187-8531, JAPAN*
akutag-k@bridgestone.co.jp, tnishi@polymer.titech.ac.jp

NEDO has carried out a new program with industries and academia to develop super fuel-efficient tire materials between 2009–2011. The program focuses on the design of tire compound with three-dimensional nano-hierarchial architecture optimized for super fuel-efficient tires. It aims not only to reduce rolling resistance but also to solve the trade -off between rolling resistance and wear performance. Computational science and imaging techniques were extensively used to design and control the nano-architecture of the tire compound. The virtual simulation of the nano-architecture gives us ideas that have never been realized in compound design[1].

For this project we have proposed new characterization methods for three-dimensional nano-scale hierarchical architecture, which can be divided into three different scale ranges: 10nm with crosslinks, 100nm with filler dispersion and 1000nm with polymer blends. The 3D-TEM and AFM were developed to derive the 3D image of actual nano-hierarchial architecture and the distribution of mechanical properties in nano-scale, respectively. These techniques were developed working together with special members organized under the NEDO program. These methods can enable us to visualize the mechanical behavior of the compound under deformation with stress concentration in nano-scale[2].

The technology can be applied not only to complex elastomeric materials but also to polymer alloys, blends, and composites. In this invited lecture we will introduce some of the main concepts and results of the project since it is very complex and there are many members from industry and academia.

Visualization of crosslink network structure

The crosslink network in 3D was visualized with combination of 3D-TEM and the Shi-ibashi method, which is a technique of special pretreatment for the visualization of the crosslinks of cured rubbers[3]. The specimen was prepared with the crosslinked rubber swollen with styrene monomer which was polymerized after swelling. The crosslinked rubber chain was stained and visualized by 3D-TEM. The 3D structural image of crosslink network is shown in Fig. 1, which was processed with the thinning image software. The reconstructed image in 3D was divided into cubical cells and calculated the volume fraction of rubber at each cell. The crosslink density of each cell was calculated using Flory-Rehner equation and the modulus were calculated. The histogram of the modulus is also shown in Fig. 1, where it is found that the modulus in nano-scale are widely distributed[2].

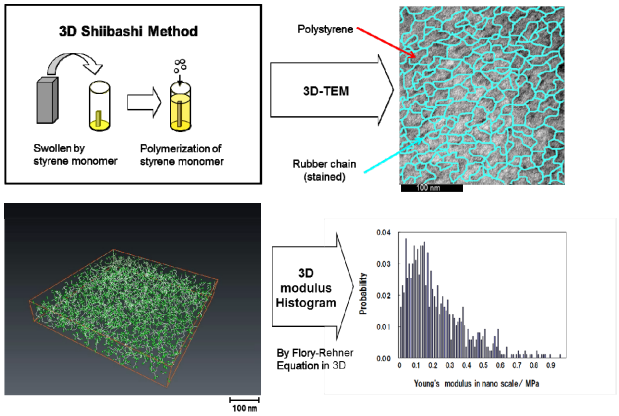

Fig. 1. **Visualization of 3D crosslink network using Shi-ibashi method[2]**

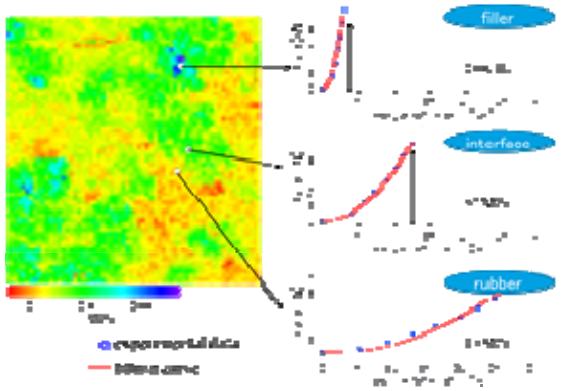

Fig. 2. **Young's modulus distribution of filled rubber using nano-mechanical mapping technology[4]**

Young's modulus mapping of filled rubber

Atomic force microscopy (AFM) was applied to visualize topographic and mechanical properties in nano-sscale. Young's modulus can be derived with nano-scale resolution by means of analyzing the force-distance curve with Hertz theory. Young's modulus distribution of filled rubber with this method are shown in Fig. 2. It can be recognized that the magnitude of modulus can be divied into three regions; rubber, carbon black (or bound rubber) and interfacial regions[4].

3D distribution of fillers

The filler network structure in nano-scale was visualized by 3D-TEM (ref.[5]). The advantage of this method is direct observation of filler network without any pretreatment such as etching of the filled rubber. The complicated structure of filler network can be seen and was combined with voxel method to construct the 3D finite element model in nano-scale[6]. The reconstructed filler network image and its digitized sheet were shown in Fig. 3.

Finite element analysis in mesoscopic scale and nano-mechanical simulation

The model is transferred into finite element analysis software and stretched in uni-axial direction up to 15 % strain. In each strain step, the stress and strain energy density are calculated for each voxel. Overall stress and strain energy density are calculated by sum of all voxels data. From strain energy data, Young's modulus is calculated and this data is compared with experimental data as shown in Fig. 5. To the first approximation, Young's modulus calculated from FEM shows a good agreement with the experimental data, and the magnitude is 4 times higher than that of unfilled rubber. This gap is thought to be a Payne effect and volume effect by filler incorporation in rubber. Also shown in the sliced images of Fig. 5, color graduation represents the strain distribution in rubber under strain. Dark blue colored pixel represents zero deformation and red colored pixel represents strain over

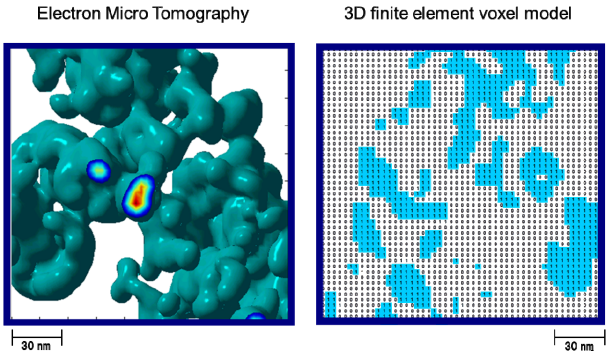

Fig. 3. **Visualization of filler network using 3D electron micronto-mography and its digitized image for 3D finite element voxel model[6]**

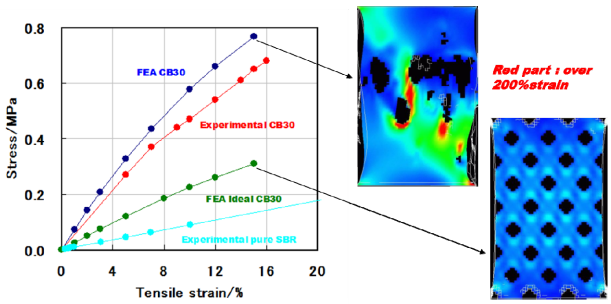

Fig. 4. **Stress-strain curves of calculated and measured results with sliced images. FEA CB30:actual rubber, FEA Ideal CB30:virtual rubber and Experimental CB30:measured**

100 %. Strain distribution is not uniform and even if overall strain is 15 %, red colored position which shows over 200 % of strain can be seen.

Nano hierarchical structure control for super fuel-efficient tire rubber

The finite element method in nano-scale was used to determine the ideal nano-hierarchical architecture to solve the trade-off between rolling resistance and wear performance as described in Fig. 5. For A-B polymer blend architecture the phase A with high wear toughness and the phase B with low energy loss should be placed together in nano-scale. For filler architecture the filler particle should be placed in highly dispersed state. For cross-link network architecture the cross-link points should be distributed uniformly. Three steps of nano-architecture control technologies were applied to satisfy these preconditions of the ideal nano-hierarchical architecture. The optimization of polymer blend improved wear with 60 %, the improvement of filler dispersion reduced the energy loss with 52 % and the optimization of the crosslink network gave additional improvement in energy loss with 12 %. As a result the compound optimized in nano-hierarchical architecture was able to satisfy the target performances of balance between energy loss and wear.

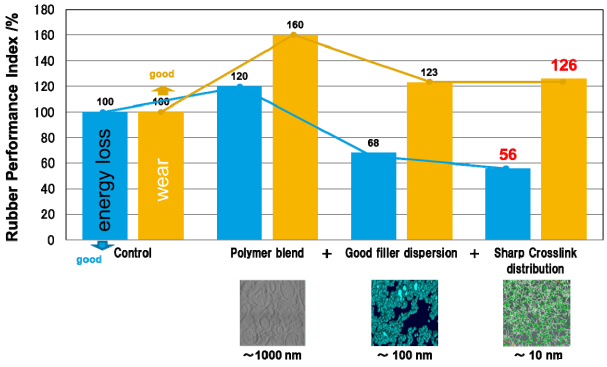

Fig. 5. **Nano-architecture design steps to solve trading-off between energy loss and wear properties of tread compounds[2]**

Conclusion

1. Nano-structure visualization methods were developed by collaboration between industry and academia with a project supported by NEDO.
2. Nano-hierarchical structure controls such as good dispersion of filler and sharp distribution of crosslink density can give lower energy loss, which is necessary for fuel-efficient tires.
3. Nano visualization technologies are found to be useful to design the nano-architecture, especially for the development of the super fuel-efficient and better wear tires.

We are grateful for the support of New Energy and Industrial Technology Development Organization NEDO. We also would like to thank Bridgestone Corporation, WPI-AIMR Tohoku University (Prof. Ken Nakajima), IMCE Kyushu University (Prof. Hiroshi Jinnai), AIST (Dr. Hiroshi Morita), and JSR Corporation (Mr. Takuo Sone) for their cooperation.

REFERENCES

1. Akutagawa K.: *Tire Technology EXPO Conference Program,* Day 1, Feb. 5, 2013, Koeln Messe, Germany.
2. Nishi T.: *Tire Technology EXPO Conference Program,* Day 1, Feb. 5, 2013, Koeln Messe, Germany.
3. Shi-ibashi T., Hirose K., Tagata N.: Kobunshi Ronbunshu *46*, 473 (1989).
4. Nishi T., Nukaga H., Fujinami S., Nakajima K.: Chinese J. Polymer Sci. *25*, 1 (2007).
5. Jinnai H., Shinbori Y., Kitaoka T., Akutagawa K., Mashita N., Nishi T.: Macromolecules *40*, 6758 (2007).
6. Akutagawa K., Yamaguchi K., Yamamoto A., Heguri H., Jinnai H., Shinbori Y.: Rubber Chem. Technol. *81*, 182 (2008).

ML-03
POLYMER BLENDS AND NANOCOMPOSITES FOR AUTOMOTIVE APPLICATIONS

Appropriately formulated blends of polypropylene (PP) with ethylene-octene elastomers (EOR), organoclays based on montmorillonite (MMT) clays and a maleated PPcan lead to Thermoplastic Olefin (TPO) materials with better toughness and stiffness that are suitable for many automotive applications.

RAJKIRAN TIWARI and DONALD R. PAUL*

University of Texas at Austin, Department of Chemical Engineering, Austin, Texas 78712 USA

Elastomer particle size has a significant effect on the impact strength of rubber-toughened thermoplastics. We have shown that the size of ethylene-co-octene elastomer, EOR, particles are significantly reduced by the addition of organoclay based on montmorillonite, MMT, and as the molecular weight of the polypropylene, PP, matrix is increased . The high shear stress exerted by the PP matrix and the inhibition of coalescence of elastomer particles caused by the MMT facilitate this decrease in the elastomer particle size .In addition, the elastomer particle size is also affected by the elastomer rheology, i.e., melt flow index, MFI, and octene content of the elastomer. The EOR particles are mostly elongated in shape due to deformation during the injection molding process .

The matrix molecular weight is known to influence the mechanical properties and toughness of rubber-toughened blends; this is related to the inherent ductility of the matrix and its response to toughening for different elastomers. However, little is known in particular for extruder-made TPO

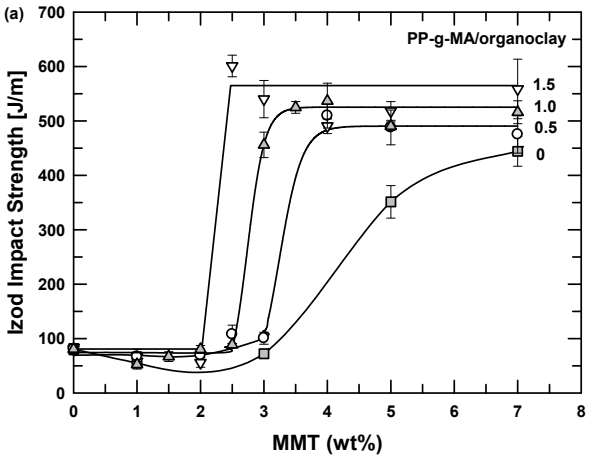

Fig. 1. **Effect of MMT and PP-g-MA on the room temperature Izod impact strength of a PP/EOR blend**

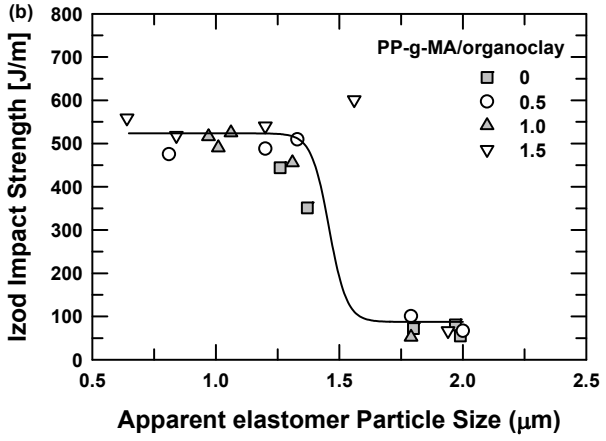

Fig. 2. **The combined effects of MMT and PP-g-MA content translate into an effect of EOR particle size which controls the Izod impact strength**

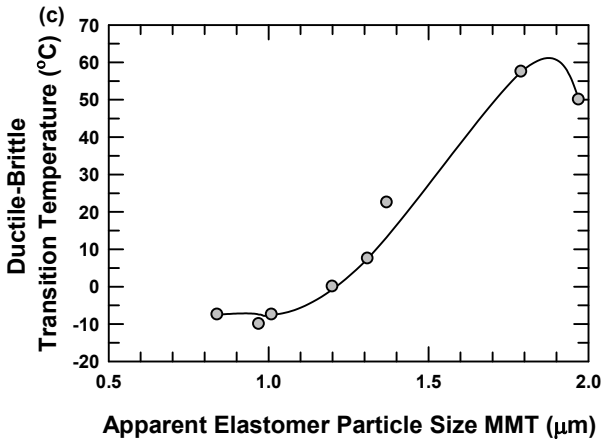

Fig. 3. **The reduction in EOR elastomer particle size by addition of MMT and controlling the PP-gMA content reduces the ductile-brittle transition temperature of PP/EOR blends**

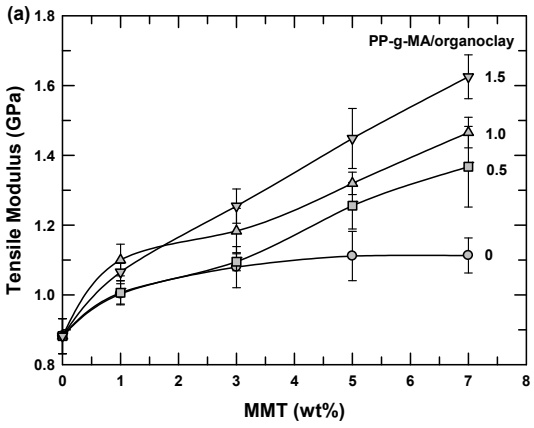

Fig. 4. **Addition of MMT increases the modulus of the PP/EOR blends as does increasing the PP-g-MA content**

nanocomposites about how the PP molecular weight, elastomer type, and MMT content affect the elastomer particle size and toughness. This is important since nanocomposites with a good balance of toughness and stiffness have many potential applications. Extruder-made TPO blends from low MFI PP (< 1g/10 min @ 190 °C) have shown toughness > 600 J m^{-1}; however, applications of such blends are limited due to processibility issues arising from high matrix viscosity; on the other hand, controlling elastomer particle size using MMT provides a unique combination of toughness and stiffness even for low molecular weight PP useful for injection molding[24].

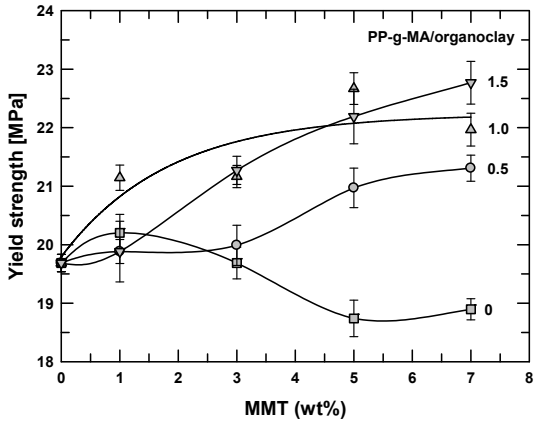

Fig. 5. **Increasing the MMT and PP-g-MA content increases the yield strength of the PP/EOR blend**

This paper explores the combined effects of elastomer particle size along with the molecular weight of PP, elastomer MFI, elastomer octene content and MMT content on the toughness of extruder-made PP/PP-g-MA/MMT/EOR nanocomposites. The room temperature Izod impact strength is examined to separate out effects of each parameter on the toughness of the PP/PP-g-MA/MMT/EOR nanocomposites. The effects of elastomer particle size and PP molecular weight on impact strength are reported. The tensile modulus and yield strength are shown to increase with MMT content. The extruder-made TPO nanocomposite provides a favorable balance of properties relative to a commercial reactor-made TPO nanocomposite. The results from this study should be useful for developing formulations of extruder-made TPOs in terms of elastomer particle size control and toughness, based on end-use applications.

The property enhancements that are possible by this strategy are illustrated in Figures 1–5.

Further details about this investigation can be found in the following references[1–5].

REFERENCES

1. Tiwari R.R., Paul D.R.: Polymer. *52*, 4955 (2011).
2. Tiwari R.R., Paul D.R.: Polymer. *52*, 5595 (2011).
3. Tiwari R.R., Paul D.R.: Polymer. *53*, 823 (2012).
4. Tiwari R.R., Paul D.R.: J. Polym. Sci., Part B: Polym. Phys. *50*, 1577 (2012).
5. Tiwari R.R., Paul D.R.: J. Polym. Sci., Part B: Polym. Phys. In press.

ML-04
NANOTECHNOLOGY AND CARBON FIBRE IN GREEN COMPOSITES

MOHINI MOHAN SAIN

Centre for Biocomposites and Biomaterials Processing, University of Toronto, 33 Willcocks Street, Toronto, Canada
m.sain@Utoronto.ca

ML-05
CNT-RUBBER INTERACTION – A BASE FOR INNOVATIVE RUBBER MATERIALS

ROBERT H. SCHUSTER *, H. CHOGULE, and H. WITTEK

Deutsches Institut f. Kautschuktechnologie, Eupener Str. 33, 30519 Hannover
Robert.Schuster@DIKautschuk.de

Over the last decade carbon nanotubes (CNTs) have been the subject of intense investigations in both fundamental and applied science[1]. Due to outstanding mechanical strength, sur-face specific area, aspect ratio and electrical properties CNTs are promising candidates to produce polymeric nano-compo-sites with outstanding mechanical properties and high electrical conductivity. The challenge in achieving the desired goals is to find suitable processing strategies for efficient CNT dispersion in the polymer matrix[2]. In many studies CNTs are incorporated into the polymer via suspensions in fluids and sonication followed by solvent evaporation[3].

The contribution aims to investigate application oriented strategies for CNT dispersion by mechanical mixing and latex compounding into rubbers with different but defined chemical constitution (NR, NBR, HNBR, EVA, EPDM, Q and FKM). The experimental series have been carried out using four different types of Multiwalled Carbon Nanotubes (MWCNT): Nanocyl (NC) NC7000, NC3100 and Baytubes (BT) C150HP and C70P.

The focus is to emphasize the effect of CNT dispersion on polymer chain dynamics, transport phenomena, mechanical reinforcement and ultimate properties. In addition the impact of CNTs on rubbers mixes filled with high loadings of well dispersed carbon black and/or silica was investigated (hybrid systems) as an option for short term applications of CNTs in elastomeric products.

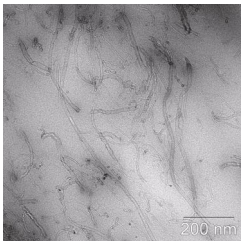

Fig. 1. **CNT dispersion**

Master batches with up to 5 vol.% CNT were prepared by (i) dry melt mixing using a laboratory internal mixer at variable rotor speed and mixing time, (ii) subsequent mixing on a two-roll mill, (iii) extrusion through a special die and (iv) latex compounding.

By dry melt mixing a good dispersion and random distribution of MWCNTs is observed. High shear rates and prolonged mixing on the two roll-mill lead to a better homogeneity but also to a break-down of the tube length and a lower aspect ratio. By the technique of latex compounding good dispersion was obtained.

It is shown that the electrical percolation threshold is influenced (i) by the chemical nature of the polymer, (ii) the type of the CNT and the process parameters that control the dispersion. For constant mixing conditions in the internal mixer (20 min.) the following sequence of electrical percolation thresholds (in vol.% CNTs) was established:

NR (1.0)< FKM(1.3)<Q(1.5)<NBR(1.5)<HNBR(1.8)

Keeping the mixing conditions at constant it was observed that the electrical percolation threshold decreases with the polarity of the polymer indicating specific interactions. The percolation threshold increases with the tube diameter and the entangle-ment density of the CNTs. Furthermore the saturation conductivity systematically higher for polymers with lower percolation limits and reach conductivity values up to 1S/cm.

Crosslinked CNT/Rubber nanocomposites demonstrate similar dynamic-mechanical properties as CB filled elastomers but at far less volume fraction of the filler. Due to the strong polymer-CNT interaction and the high degree of dispersion the “Payne-Effect” is less pronounced than in CB filled elastomers. Consequently the nanocomposites demonstrate lower hystere-sis and higher elasticity at the same hardness or stiffnes of the systems.

The reinforcement by CNTs is clearly seen in the increase of the stress in the strain region up to 300 % as well as in the non -linear increase of the tensile strength as a function of the CNTs content This level of reinforcement cannot be achieved by CB or silica. For CNTs with a small tube diameter the reinforcing effects are considerably higher than for ones with large tube diameter. The effect is attributed to the higher polymer-filler contact surface per unit volume and to the higher surface activity due to more pyramidalization[4].

If the normalized stress at a given elongation is considered as a criteria for reinforcement the plotted curves

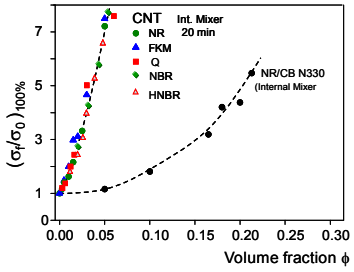

Fig. 2. **Reinforcing factor for CNT- and CB-systems**

for all the systems under investigation demonstrates that the intrinsic reinforcing mechanism depends primarily on the CNTs and their state of dispersion (Fig. 2).

Remarkable improvements of the mechanical properties were observed for hybrid nanocomposites. The addition of small con-centrations of CNTs to CB filled compounds increases the Young's modulus, stress values, tear energy and dyna-mical cut growth resistance significantly.

The authors acknowledge the support given by the BMBF within the InnoCNT Allianz.

REFERENCES

1. S. B. Sinnot, R. Andrews: Crit. Rev. Solid State Mater. Sci. *26*, 145 (2001).
2. M. M. J. Treacy, T. W. Ebbesen: Nature *382*, 678 (1996).
3. L. Bokobza, M. Rahmani: KGK, Kautsch. Gummi Kunstst. *62*, 112 (2009).
4. X. Lu, Zh. Chen: Chem. Rev. *105*, 3643(2005).